13

Application of Finite Element Analysis in Sheet Material Joining

Xiaocong He
Kunming University of Science and Technology, PR China

1. Introduction

Lightweight construction strategies have become increasingly important in recent years for economic reasons and in terms of environmental protection. Some sheet material joining techniques, such as self-pierce riveting, mechanical clinching and structural adhesive bonding, have been developed for joining advanced lightweight sheet materials that are dissimilar, coated, and hard to weld (He et al., 2008, He, 2010b, 2011b, 2012).

Traditionally, the mechanical behavior of a sheet material joint can be obtained by closed-form equations or experiments. For a fast and easy answer, a closed-form analysis is appropriate. However, the mechanical behavior of sheet material joints is not only influenced by the geometry of the joints but also by different boundary conditions. The increasing complex joint geometry and its three-dimensional nature combine to increase the difficulty of obtaining an overall system of governing equations for predicting the mechanical properties of sheet material joints. In addition, material non-linearity due to plastic behavior is difficult to incorporate because the analysis becomes very complex in the mathematical formulation. The experiments are often time consuming and costly. To overcome these problems, the finite element analysis (FEA) is frequently used in sheet material joints in recent years. The FEA has the great advantage that the mechanical properties in a sheet material joint of almost any geometrical shape under various load conditions can be determined.

For having a knowledge of the recent progress in FEA of the sheet material joints, latest literature relating to FEA of sheet material joints is reviewed in this chapter, in terms of process, strength, vibration characteristics and assembly dimensional prediction of sheet material joints. Some important numerical issues are discussed, including material modeling, meshing procedure and failure criteria. It is concluded that the FEA of sheet material joints will help future applications of sheet material joining by allowing system parameters to be selected to give as large a process window as possible for successful joint manufacture. This will allow many tests to be simulated that would currently take too long to perform or be prohibitively expensive in practice, such as modifications to joint geometry or material properties. The main goal of the chapter is to review recent progress in FEA of sheet material joining and to provide a basis for further research.

2. FEA of self-pierce riveting

Self-pierce riveting (SPR) is used for high speed mechanical fastening of sheet material components. In this process, a semi-tubular rivet is pressed by a punch into two or more substrates of materials that are supported on a die. The die shape causes the rivet to flare inside the bottom sheet to form a mechanical interlock as shown in Fig. 1. Fig. 2 shows the SPR machine and the SPR tools in Innovative Manufacturing Research Centre of Kunming University of Science and Technology.

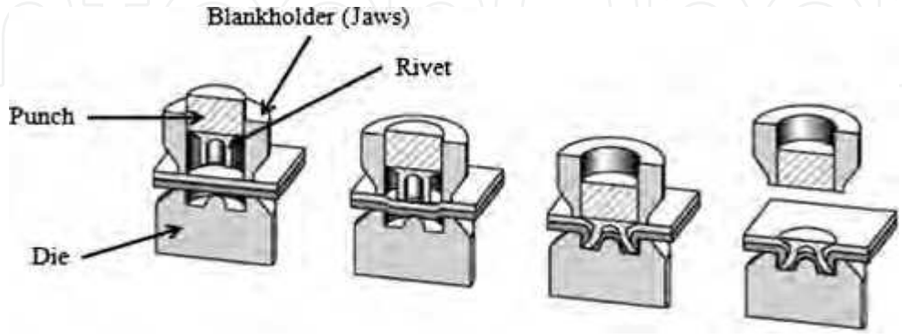

Fig. 1. SPR operation with a semi-tubular rivet.

Fig. 2. SPR machine and SPR tools.

2.1 SPR process

It is very difficult to get insight into the joint during forming process due to the complicacy of the SPR process. The effective way to analyze SPR joint during forming process is to perform finite element simulation. Several numerical techniques and different FEA software already allows the simulation of the SPR process.

The riveting process has been numerically simulated using LS-DYNA (Yan et al., 2011). A 2D axi-symmetric model was used with an implicit solution technique encompassing 'r-adaptivity' and geometrical failure based on the change in thickness of the substrates. An extensive experimental program using aluminum alloy 5052 substrates generated a database for the validation of the numerical simulations. Good agreements between the simulations and laboratory test results were obtained, for both the force/deformation curves and the deformed shape of the rivet and substrates. Fig. 3 shows the FE simulation of the SPR process and Fig. 4 shows the cross section comparison between simulation and test.

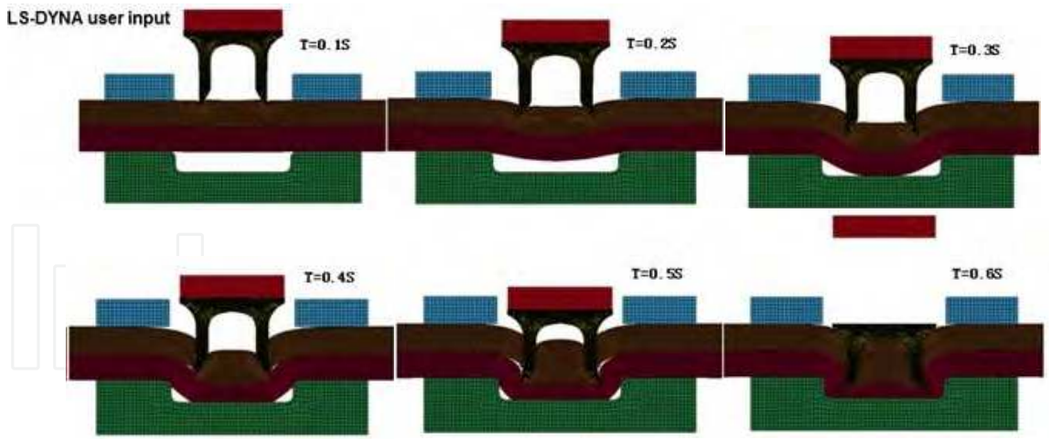

Fig. 3. FE simulation of the SPR process (Yan et al., 2011).

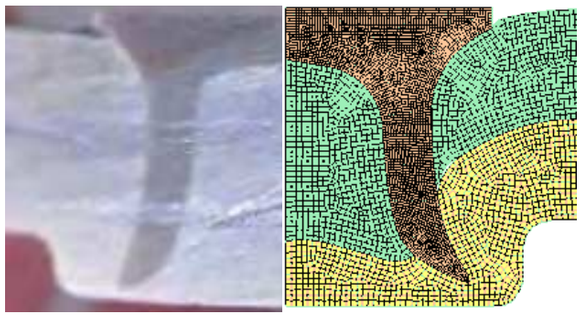

Fig. 4. Cross-section comparison between simulation and test (Yan et al., 2011).

A study (Abe et al., 2006) investigated the joinability of aluminum alloy and mild steel with numerical and test results. The joining process was simulated by LS-DYNA 2D axi-symmetric models. To shorten the calculation time for this explicit dynamic FEA code, the punch velocity was increased to about 25 times the real speed used for riveting. In this study, defects in the process were categorized as either penetration through the lower sheet, necking of the lower sheet or the separation of substrates (caused by different strains when substrates are made of different materials). The authors concluded that these defects were caused by the small total thickness, the small thickness of lower sheet and the large total thickness, respectively.

Mori et al. (Mori et al., 2006) developed an SPR process for joining ultra-high-strength steel and aluminum alloy sheets. To attain better joining quality, the die shape was optimized by means of the FEA without changing mechanical properties of the rivet. Authors reported that the joint strength is greatly influenced by not only the strength of the sheets and rivets but also the ratio of the thickness of the lower sheet to the total thickness. Abe et al. (Abe et al., 2009) investigated the effects of the flow stress of the high-strength steel sheets and the combination of the sheets on the joinability of the sheets by FEA and an experiment. They found that as the tensile strength of the high-strength steel sheet increases, the interlock for the upper high-strength steel sheet increases due to the increase in flaring during the driving through the upper sheet, whereas that for the lower high-strength steel sheet decreases.

A 3D model was created by Atzeni et al. (Atzeni et al., 2007) in ABAQUS Explicit 6.4 and both the SPR process and the shear tests were simulated to take into account the strain and residual stress of the SPR joints. Comparisons with experimental results had shown good agreement, both in terms of deformed geometry and force-displacement curves. In another study, the same authors (Atzeni et al., 2009) presented a FEA model for the analysis of the SPR processes. Correct model parameters were identified and numerical model validated in 2D simulations. In order to verify the capabilities of the software to predict joint resistance for given geometry and material properties, a 3D model was set up to generate a joint numerical model for simulating shearing tests. In Kato et al.'s paper (Kato et al., 2007), a SPR process of three aluminum alloy sheets was simulated using LS-DYNA to find joinable conditions. In addition, the cross-tension test was also simulated by FEA to evaluate the joint strength.

Using Forge2005® FE software, Bouchard et al. (Bouchard et al., 2008) modeled large deformation of elastic–plastic materials for 2D and 3D configurations. They found that it is possible to export the mechanical fields of a 2D simulation onto a 3D mesh using an interpolation technique, and then to perform a 3D shearing test on the riveted structure. They also found that the mechanical history of the rivet/sheet assembly undergone during the SPR process plays a significant role in the numerical prediction of the final strength of the assembly. In order to evaluate the software robustness, numerical simulation of the SPR process was performed on three 1-mm-thick aluminum and steel sheets. Fig. 5 shows the four different stages of the SPR process of three sheets.

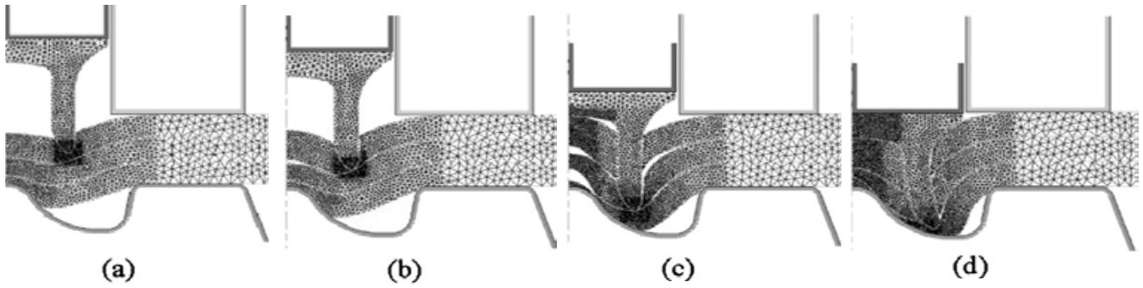

Fig. 5. Four different stages of the SPR of three sheets (Bouchard et al., 2008).

Casalino et al. (Casalino et al., 2008) proposed equations for governing the onset and propagation of crack, the plastic deformation, the space discretization, the time integration, and the contact evolution during the SPR process. A case study of the SPR of two sheets of the 6060T4 aluminum alloy with a steel rivet was performed using the LS-DYNA FE code. Some numerical problems entangled with the model setup and running were resolved and good agreement with experimental results was found in terms of joint cross-sectional shape and force–displacement curve. Fig. 6 shows the initial and final configuration of the joint.

The SPR process currently utilizes high-strength steel rivets. The combination between steel rivets with an aluminum car body not only makes recycling time consuming and costly, but also galvanic corrosion. Galvanic corrosion occurs when dissimilar, conductive materials are joined and the ingress of water forms an electrolytic cell. In this type of corrosion, the material is uniformly corroded as the anodic and cathodic regions moves and reverses from time to time (He et al., 2008). Hoang et al. (Hoang et al., 2010) investigated the possibility of

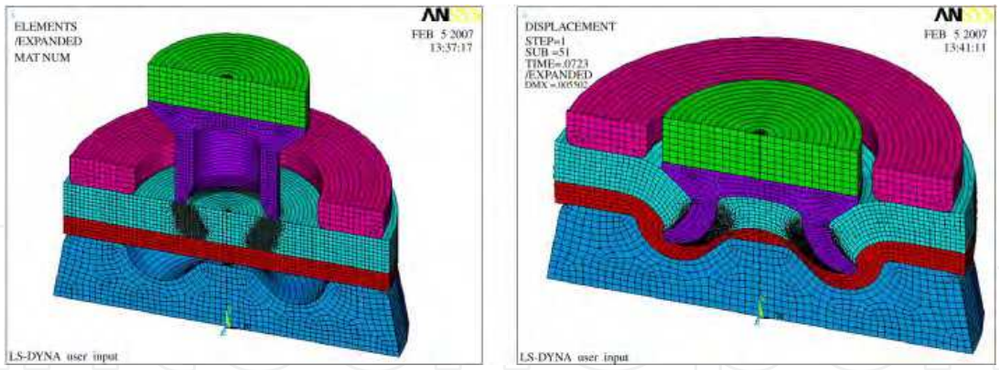

Fig. 6. Initial and final configuration of the joint (Casalino et al., 2008).

replacing steel self-piercing rivets with aluminum ones, when using a conventional die in accordance with the Boellhoff standards. An experimental program was carried out. The test results were exploited in terms of the riveting force–displacement curves and cross-sectional geometries of the riveted joints. The test data were also used to validate a 2D-axisymmetric FEA model. The mechanical behavior of a riveted connection using an aluminum rivet under quasi-static loading conditions was experimentally studied and compared with corresponding tests using a steel rivet.

2.2 Static and fatigue behavior of SPR joints

Sheet material joints are often the structural weakest point of a mechanical system. Consequently a considerable amount of FEAs have been carried out on the static and fatigue behavior of SPR joints. As SPR is considered to be an alternative to spot welding, most research studies have focused on comparisons of the mechanical behavior of joints manufactured by these techniques. Research in this area has shown that SPR gives joints of comparable static strength and superior fatigue behavior to spot welding, whilst also producing promising results in peel and shear testing. Fig. 7 compares the fatigue behavior of three typical joining techniques (Cai et al., 2005).

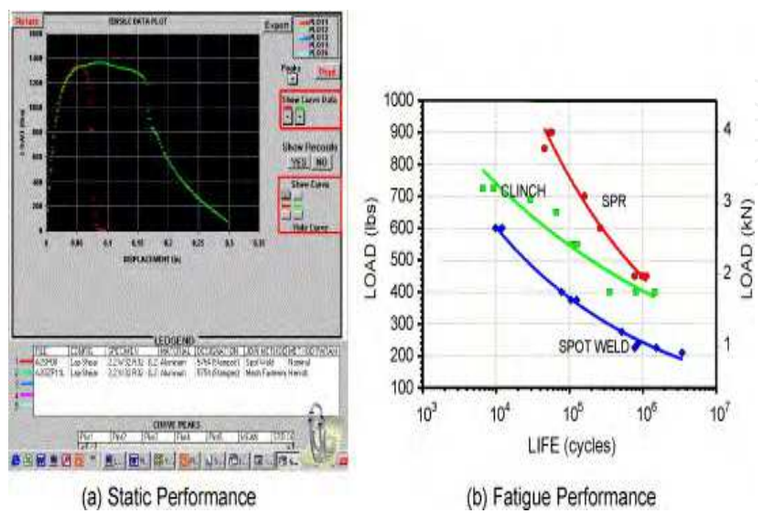

Fig. 7. Fatigue behavior comparison of SPR, clinching and spot welding (Cai et al., 2005).

The fatigue behavior of single and double riveted joints made from aluminum alloy 5754-O has been studied by Iyer et al. (Iyer et al., 2005). A 3D elastic FEA showed that crack initiation occurred at the region of maximum tensile stress. This finding highlights the importance of the cold-formed geometric nonlinearities in determining joint's mechanical strength. The authors also found that both the fatigue and static strength of double-riveted SPR joints was strongly dependent on the orientation (direction that the rivet is inserted; either both from the same side or one from each side) combination of the rivets. The study shows that the analyses were useful for interpreting experimental observations of fatigue crack initiation location, life and fretting damage severity.

Porcaro et al. (Porcaro et al., 2004) developed a numerical model of a riveted structure with the finite element code LS-DYNA to investigate the behavior of a single-riveted joint under combined pull-out and static shear loading conditions. The rivet was represented using the *CONSTRAINED_SPOTWELD card and included failure criteria based on a critical plastic failure strain and the force envelope. Validation was achieved from static and dynamic laboratory test results. The numerical analyses of these components provided a direct check of the accuracy and robustness of the numerical model. The same authors also generated an accurate 3D numerical model of different types of riveted connections, subjected to various loading conditions (Porcaro et al., 2006). An algorithm was generated in order to transfer all the information from the 2D numerical model of the riveting process to the 3D numerical model of the connection. Again the model was validated against the experimental results.

Kim et al. (Kim et al., 2005) tried to evaluate the structural stiffness and fatigue life of SPR joint specimens experimental and numerically by FEA modeling in accordance with the FEMFAT guidelines. The authors found that even though the joint stiffness was independent of substrate thicknesses, the fatigue life was dependant on substrate material and thickness. In research paper of Galtier and Duchet (Galtier & Duchet, 2007), the main parameters that influence the fatigue behavior of sheet material assemblies were presented and some comparisons were made within sheet material joining techniques. It was found that the SPR joint fatigue strength mainly depends on the grade and thickness of the sheet placed on the punch side. In Lim's research paper (Lim, 2008), the simulations of various SPR specimens (coach-peel specimen, cross-tension specimen, tensile-shear specimen, pure-shear specimen) were performed to predict the fatigue life of SPR connections under different shape combinations. FEA models of various SPR specimens were developed using a FEMFAT SPOT SPR pre-processor.

The SPR process has the disadvantage of needing high setting forces typically around 10 times those used for spot-welding. This large setting force can cause severe joint distortion and this will affect the assembly dimensions. SPR joint distortion was found to be much larger, about two to four times the magnitude, than that from resistance spot welding. It was suggested that the inclusion of SPR joint distortion is generally needed for accurate global assembly predictions. To include this localized SPR effect, Sui et al. (Sui et al., 2007) has built a FE model for simulating SPR process of 1.15 mm AA6016T4+1.5 mm AA5182O sheets. The results show that punching load was significantly affected by the deformation of rivet shank and the distortion of the joints was mainly affected by the binder force and the blankholder diameter.

The structural behavior of the SPR joints under static and dynamic loading conditions and how they are modeled in large-scale crash analyses are crucial to the design of the overall structure. Therefore, there is a need to perform dynamic testing on elementary joints in order to study its dynamic behavior. Porcaro et al. (Porcaro et al., 2008) investigated the SPR connections under quasi-static and dynamic loading conditions. Two new specimen geometries with a single rivet were designed in order to study the riveted connections under pull-out and shear impact loading conditions using a viscoelastic split Hopkinson pressure bar. 3D numerical simulations of the SPR connections were performed using the explicit finite-element code LS-DYNA. Static and dynamic tests were simulated using a simplified model that included only the specimen and the clamping blocks that connected the specimen to the bars.

2.3 Vibration behavior of SPR joints

Despite these impressive developments, unfortunately, research in the area of dynamic properties of the SPR joints is relatively unexplored. Hence there is a considerable need for contribution of knowledge in the understanding of the vibration characteristics of SPR joints. Research work by He et al. (He et al., 2006, 2007, Dong et al., 2010) investigated in detail the free vibration characteristics of single lap-jointed SPR beam. The focus of the analysis was to reveal the influence on the natural frequencies and mode shapes of the characteristics of the substrates. These investigations were performed by means of the 3D FEA. In order to obtain the sophisticated features such as design optimization, ANSYS Parametric Design Language (APDL) was used in the analysis. The natural frequencies (eigenvalues) and mode shapes (eigenvectors) of the free vibration of these beams were calculated for different combinations of the substrates' Young's modulus and Poisson's ratio.

By means of a parametric analysis, the influence of the Young's modulus and Poisson's ratio of the lightweight sheet materials on the natural frequencies, natural frequency ratios and mode shapes of the single lap-jointed SPR beams is deduced. Numerical examples show that the natural frequencies increase significantly as the Young's modulus of the substrates increases, but very little change is encountered for change in the substrates' Poisson's ratio. Fig. 8 shows effects of mechanical properties of sheets on torsional natural frequency. It is clear that the torsional natural frequencies increase as the Young's modulus of the sheet increases.

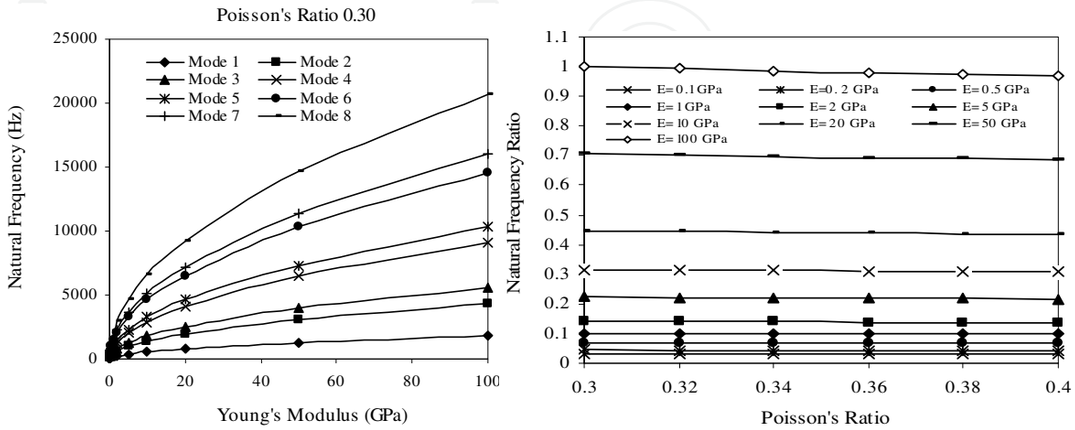

Fig. 8. Torsional natural frequencies versus Young's modulus of sheets for vs=0.30 (He et al., 2006).

Fig. 9 shows the first six mode shapes of the single lap-jointed encastre SPR beam. The mode shapes show that there are different deformations in the jointed section of SPR beams. These different deformations may cause different natural frequency values and different stress distributions. This data will enable appropriate choice of the mechanical properties of the substrates, especially Young's modulus, in order to achieve and maintain a satisfactory level of both static and dynamic integrity of the SPR structures.

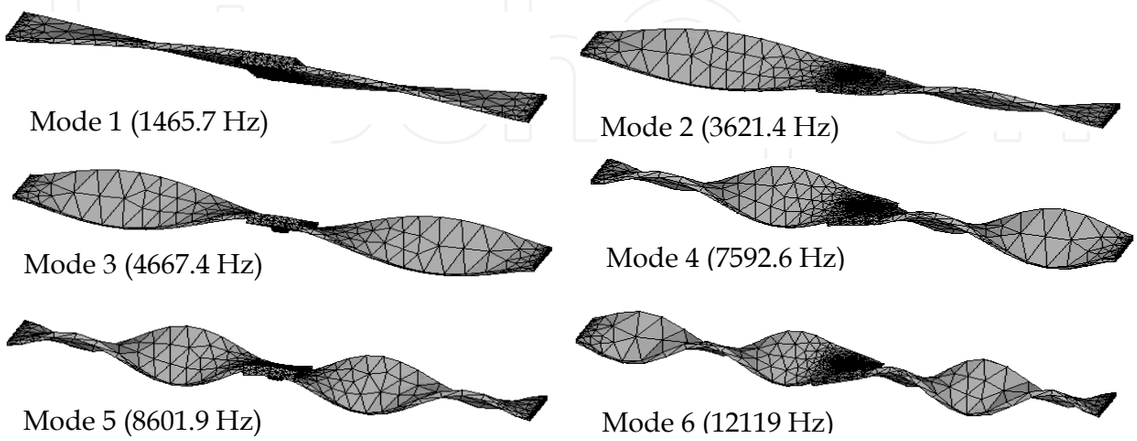

Fig. 9. First six mode shapes of the single lap-jointed SPR beam (He et al., 2006).

3. FEA of mechanical clinching

The mechanical clinching process is a method of joining sheet metal or extrusions by localized cold forming of materials. The result is an interlocking friction joint between two or more layers of material formed by a punch into a special die. Depending on the tooling sets used, clinched joints can be made with or without the need for cutting. By using a round tool type, materials are only deformed. If a square tool is used, however, both deformation and cutting of materials are required. The principle of clinching with a round tool is given in Fig. 10. Fig. 11 shows the clinching machine and clinching tools in Innovative Manufacturing Research Centre of Kunming University of Science and Technology.

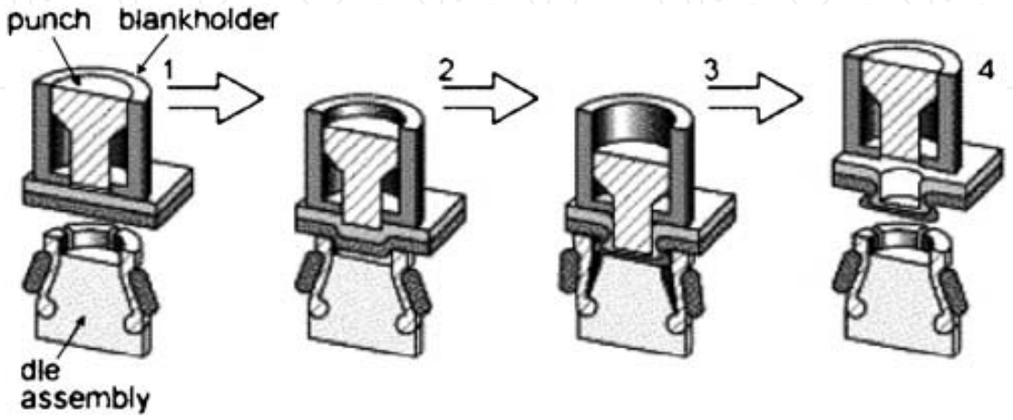

Fig. 10. Principle of clinching with a round tool.

Fig. 11. Clinching machine and clinching tools.

3.1 Clinching process

To fully understand the behavior of clinched joints, the FE model must include all the information from the clinching process. The information that can be obtained from the clinching process simulation includes: metal flow and details of die fill, distribution of strains, strain rate and stresses in the material, distribution of pressure at die–material interface, and the influence of properties like friction. The resolution of such problems is confronted with numerous nonlinear problems such as large deformations, material plasticity, and contact interactions. Several numerical techniques can be used for the simulation of such problems (dynamic or static implicit and explicit methods) and different industrial software (ABAQUS, ADINA, LS-DYNA, and MARC) already allows the simulation of the clinch forming process.

Feng et al. (Feng et al., 2011) presented a LS-DYNA 2D axi-symmetric FE model to predict the magnitude and distribution of deformation associated with the clinching process. The flow stress of the work-material was taken as a function of strain and strain rate. The shape of the clinch joint and the stress, strain, and damage in substrates were determined. Fig. 12 shows the FE simulation of the clinching process and Fig. 13 shows the cross section comparison between simulation and test.

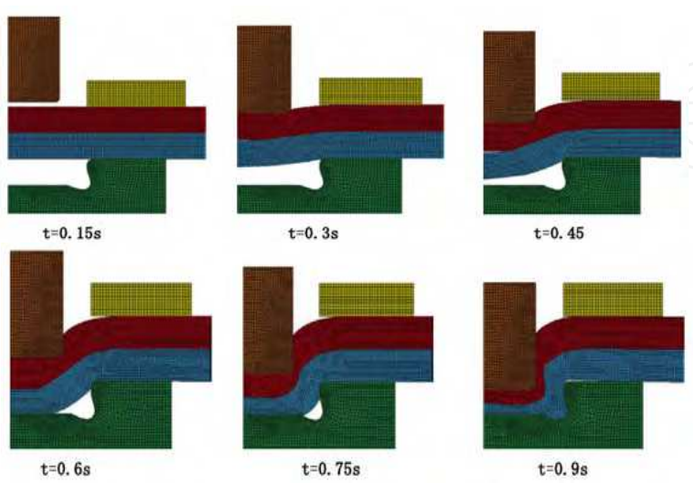

Fig. 12. FE simulation of the clinching process (Feng et al., 2011).

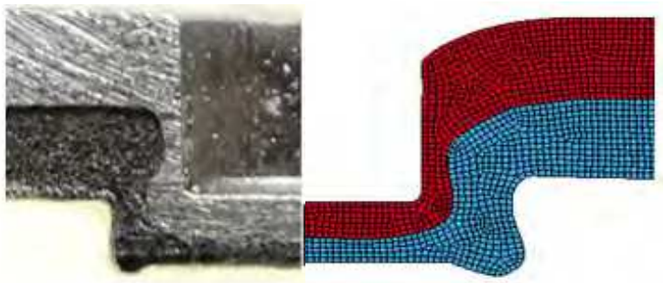

Fig. 13. Cross-section comparison between simulation and test (Feng et al., 2011).

A finite element procedure with automatic remeshing technique has been developed by Hamel et al. (Hamel et al., 2000) using ABAQUS FE software to specifically simulate the clinching process. The resolution of the updated Lagrangian formulation is based on a static explicit approach. The integration of the elastic–plastic behavior law is realized with a Simo and Taylor algorithm, and the contact conditions are insured by a penalty method. The results are compared with experimental data and numerical results calculated with a static implicit method as shown in Fig. 14.

A new clinching process, namely flat clinching, has been introduced by Borsellino et al. (Borsellino et al., 2007). After a press clinching process, the joined sheets have been deformed by a punch with a lower diameter against a flat die. In this way, a new configuration is created with a geometry that has no discontinuity on the bottom surface. Tensile tests have been done to compare the joints strength among the various clinching processes. A FEA has been performed to optimize the process.

Neugebauer et al. (Neugebauer et al., 2008) presented another new clinching method, namely dieless clinching, that works with a flat anvil as a counter tool, thus offering important benefits for the joining of magnesium. Dieless clinching allows mechanical joining of magnesium materials with very short process times because components are heated in less than 3 s. Deformation simulations with DEFORM were used to study the impact that modified punch geometry parameters have on dieless-clinched connections of various combinations of materials and component thicknesses.

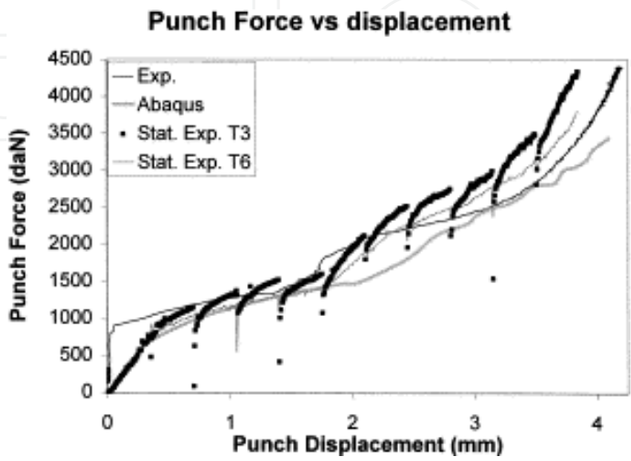

Fig. 14. Computed punch force variation (Hamel et al., 2000).

The information obtained from the process can not only lead to an improvement in die and process design achieving reduction in cost and improvement in the quality of the products but also be used to set initial parameters for a numerical model of the clinched joints used in further mechanical property studies such as static and fatigue analysis, crash analysis, and assembly dimensional prediction etc.

3.2 Strength of clinched joints

The strength of the clinching has been compared with other joining techniques, such as self-pierce riveting and spot welding by researchers (Cai et al., 2005, Lennon et al., 1999). Although the static strength of clinched joints is lower than that of other joints, but the fatigue strength of clinched joints is comparable to that of other joints, and the strength of the clinched joints is more consistent with a significantly lower variation across a range of samples.

Varis and Lepistö (Varis & Lepistö, 2003) proposed a procedure to select an appropriate combination of clinching tools, so that the maximum load under shearing test could be obtained. The calculations considered the final bottom thickness of the joint and the height of the bent area, for each of the analyzed tool combinations. FEAs were performed in order to verify the procedure, although both methods can be used either separately or together to establish optimal clinching parameters.

Carboni et al.'s work (Carboni et al., 2006) focused on a deeper study of the mechanical behavior of clinching in terms of static, fatigue, and residual strength tests after fatigue damage. Fractographic observations showed three different failure modes whose occurrence depends on the maximum applied load and on the stress ratio. Results were supported by FEA showing that the failure regions of the clinched joints correspond to those with high stress concentrations as shown in Fig. 15.

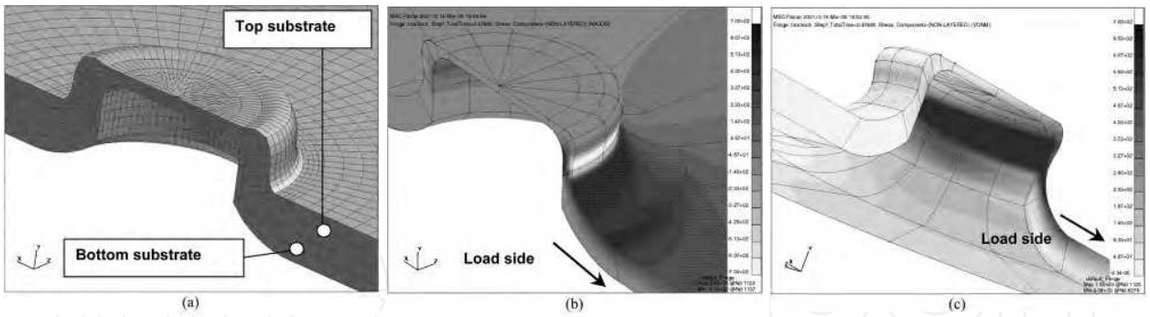

Fig. 15. FEA of clinched joints (Carboni et al., 2006): (a) brick modelling of an indentation point, (b) max principal stress in the bottom substrate and (c) maximum Von Mises stress around the neck of the indentation point.

The FEA of the clinch joining of metallic sheets has been carried out by de Paula et al. (de Paula et al., 2007). The simulations covered the effect of these changes on the joint undercut and neck thickness. The relevant geometrical aspects of the punch/die set were determined, and the importance of an adequate undercut on the joint strength was confirmed.

Clinching tools geometry optimization has been dealt systematically by Oudjene et al. (Oudjene et al., 2008). A parametrical study, based on the Taguchi's method, has been

conducted to properly study the effects of tools geometry on the clinch joint resistance as well as on its shape. The separation of the sheets is simulated using ABAQUS/Explicit in order to evaluate the resistance of clinch joints. In a similar study (Oudjene et al., 2009), a response surface methodology, based on Moving Least-Square approximation and adaptive moving region of interest, is presented for shape optimization of clinching tools. The geometries of both the punch and the die are optimized to improve the joints resistance to tensile loading. Fig. 16 shows the FEA of equivalent plastic strain distribution in a clinched joint.

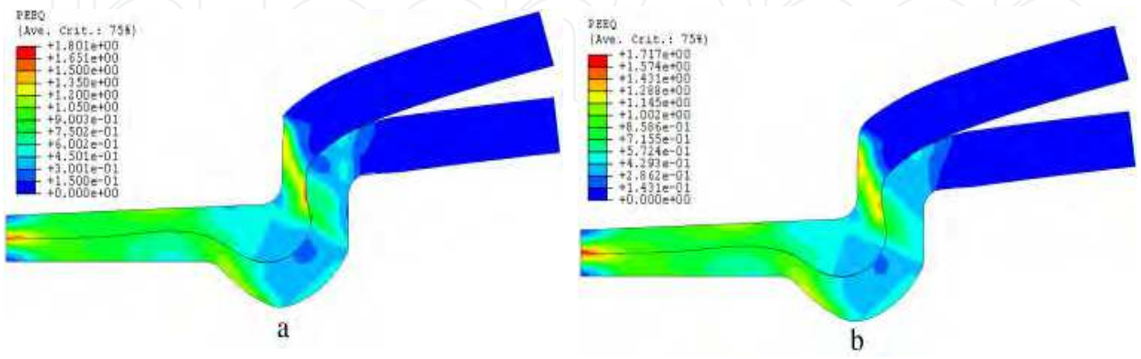

Fig. 16. Equivalent plastic strain distribution (Oudjene et al., 2009): (a) without remeshing and (b) with remeshing .

3.3 Vibration behavior of clinched joints

Mechanical structures assembled by mechanical clinching are expected to possess a high damping capacity. However, few investigations have been carried out for clarifying the damping characteristics of clinching structures and to establish an estimation method for the damping capacity.

Research papers by He et al. (He et al., 2009a, Gao et al., 2010, Zhang et al., 2010) investigated in detail the free vibration characteristics of single lap-joint clinched joints. Fig. 17 shows the first eight transverse mode shapes of the single lap-joint encastre clinched joint corresponding to material Poisson's ratio 0.33, Young's modulus 70 GPa, and density 2700 kg/m^3 (He et al., 2009a).

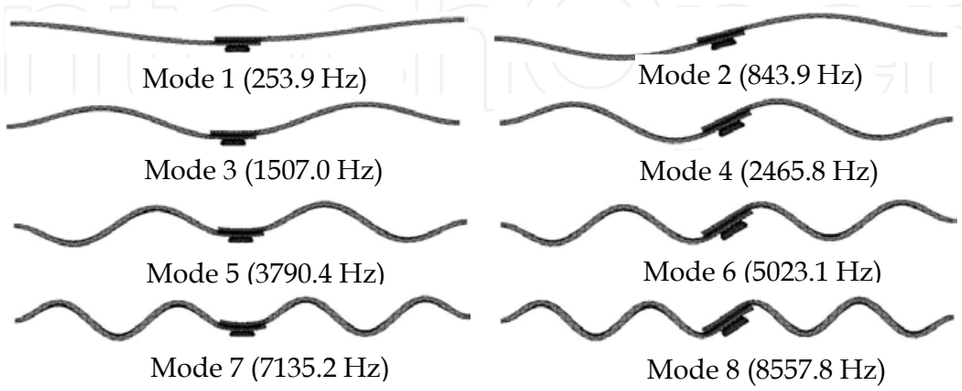

Fig. 17. First eight transverse mode shapes of the single lap-joint encastre clinched joint (He et al., 2009a).

It can be seen from Fig. 17 that the amplitudes of vibration at the midlength of the joints are different for the odd and even modes. For the odd modes (1, 3, 5, and 7), symmetry is seen about the midlength position. At these positions, the amplitudes of transverse free vibration are about equal to the peak amplitude. Thus, the geometry of the lap joint is very important and has a very significant effect on the dynamic response of the lap-jointed encastre clinched joints. Conversely, for the even modes 2, 4, 6, and 8, antisymmetry is seen about the midlength position, and the amplitude of transverse free vibration at this position is approximately zero. Hence, variations in the structure of the lap joint have relatively less effect on the dynamic response of the lap-jointed encastre clinched joints.

4. FEA of structural adhesive bonding

Adhesive bonding has come to be widely used in different industrial fields with the recent development of tough structural adhesives and the substantial improvement in the strength of adhesive joints. Up until 2009, for example, the market demand for automobile adhesives was viewed as increasing very fast and the average per-vehicle consumption of adhesives/sealants was around 20 kg. The structural automotive adhesives would have an average annual growth rate of greater than 7% over the next five years. In the aerospace industry, more and more adhesives have been used in the construction of the aircraft culminating in the Boeing 787 and the Airbus A350 both of which contain more than 50% bonded structure (Speth et al., 2010).

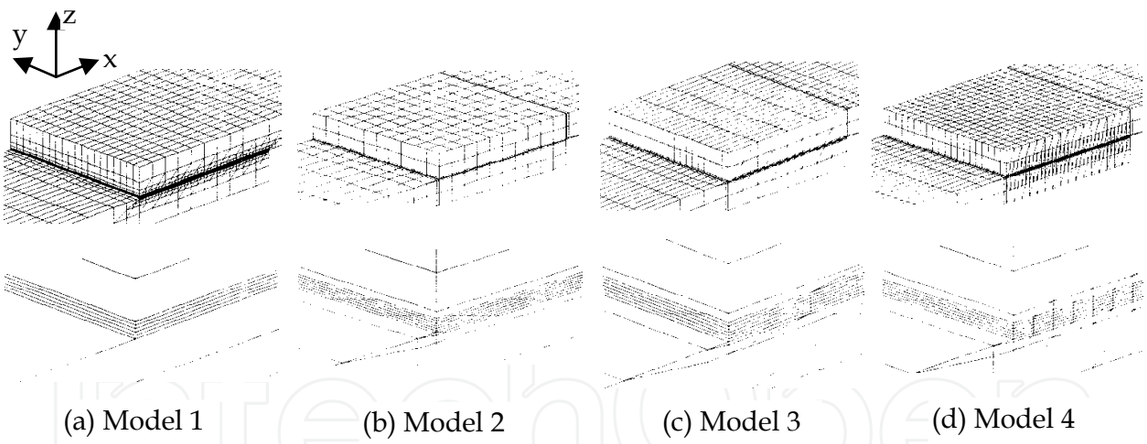

(a) Model 1 (b) Model 2 (c) Model 3 (d) Model 4

Fig. 18. Four examples of smooth transition between the adherends and adhesive (He, 2011c).

The FEA has the great advantage and is frequently used in adhesive bonding since 1970s. In the case of FEA of adhesively bonded joints, however, the thickness of adhesive layer is much smaller than that of the adherends. The finite element mesh must accommodate both the small dimension of the adhesive layer and the larger dimension of the remainder of the whole model. Moreover, the failures of adhesively bonded joints usually occur inside the adhesive layer. It is essential to model the adhesive layer by a finite element mesh which is smaller than the adhesive layer thickness. The result is that the finite element mesh must be several orders of magnitude more refined in a very small region than is needed in the rest of

the joint. Thus the number of degrees of freedom in an adhesively bonded joint is rather high. It is also important that a smooth transition between the adherends and adhesive be provided.

Some finite element models have been created by He (He, 2011c) for analyzing the behaviour of bonded joints. Fig. 18 shows four finite element models of bonded joint. From the results of the comparison of the finite element models, it is clear that within the 4 models presented here, model 3 has a moderate size of elements and nodes. Meanwhile, smooth transition between the adherends and the adhesive was also obtained in both x and z directions. Model 3 is then expected to be the best of the 4 models.

4.1 Static loading analysis of adhesive bonded joints

Adhesively bonded joints occurring in practice are designed to carry a given set of loads. The subsequent loads on the adhesive are then a function of the geometry of the joint. A common type of mechanical loading encountered by adhesively bonded joints such as in civil engineering is static loading. In addition, static analysis of adhesively bonded joints will provide a basis for further fatigue, dynamic analyses of the joints.

4.1.1 Stress distribution

The adhesively bonded joints should be designed to minimize stress concentrations. Some stresses, such as peel and cleavage, should also be minimized since these stresses are ultimately responsible for the failure of the joints. In order to determine the physical nature of stress distribution in adhesively bonded joints, the single-lap joints (SLJs) have been investigated by many researchers owing to its simple and convenient test geometry. The lap-joint problem is three-dimensional although it has a simple geometry. The stress behavior of the SLJs is rather complex since bending is induced during the deformation. It is found that the highest stresses and strain in the SLJs occur in regions at the edge of the overlap. The use of the FEA enables the distributions in the critical regions to be predicted with reasonable accuracy.

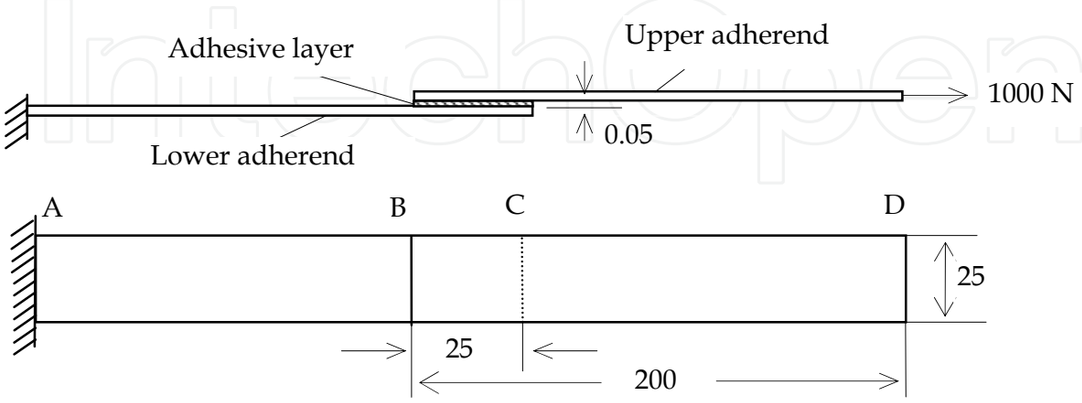

Fig. 19. A bonded joint with rubbery adhesive layer (He, 2011a).

The stress distribution in adhesively bonded joints with rubbery adhesives has been studied by He (He, 2011a). The 3-D FEA software was used to model the joint and predict the stress distribution along the whole joint. Fig. 19 shows a bonded joint with rubbery adhesive layer and Fig. 20 shows the distributions of 6 components of stresses in the lap section. The FEA results indicated that there are stress discontinuities existing in the stress distribution within the adhesive layer and adherends at the lower interface and the upper interface of the bonded section for most of the stress components. The FEA results also show that the stress field in the whole joint is dominated by the normal stresses components S_{11}, S_{33} and the shear stress component S_{13}.

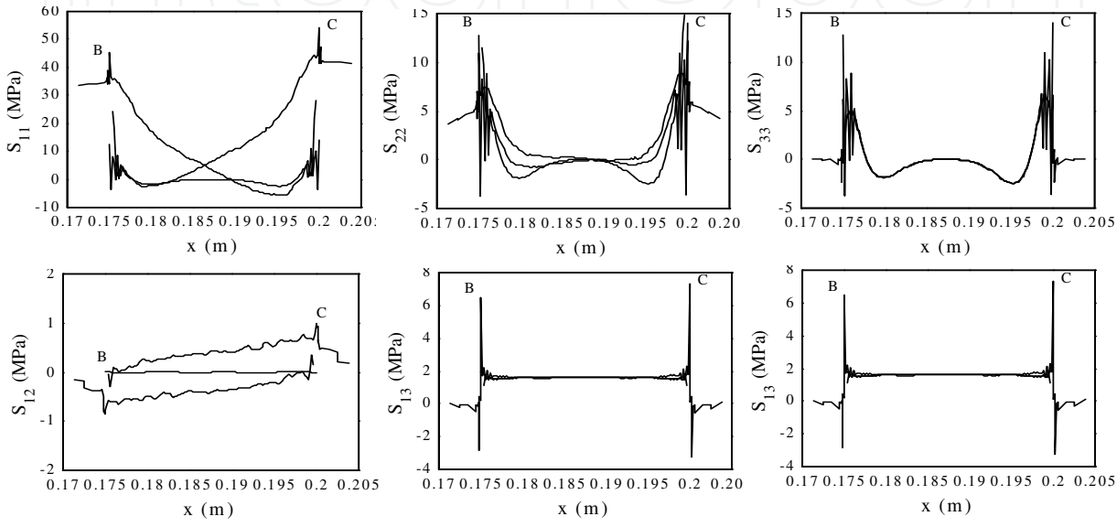

Fig. 20. Distributions of 6 components of stresses in the adhesively bonded joint (He, 2011a).

4.1.2 Stress singularity

Differences in mechanical properties between adherents and adhesive may cause stress singularity at the free edge of adhesively bonded joints. The stress singularity leads to the failure of the bonding part in joints. It is very important to analyze a stress singularity field for evaluating the strength of adhesively bonded joints. Although FEA is well suited to model almost any geometrical shape, traditional finite elements are incapable of correctly resolving the stress state at junctions of dissimilar materials because of the unbounded nature of the stresses. To avoid any adverse effects from the singularity point alternative approaches need to be sought.

Kilic et al. (Kilic et al., 2006) presented a finite element technique utilizing a global (special) element coupled with traditional elements. The global element includes the singular behavior at the junction of dissimilar materials with or without traction-free surfaces. Goglio and Rossetto (Goglio & Rossetto, 2010) explored recently the effects of the main geometrical features of an adhesive SLJ (subjected to tensile stress) on the singular stress field near to the interface end. Firstly an analysis on a bi-material block was carried out to evaluate the accuracy obtainable from FEA by comparison with the analytical solution for the singularity given by the Bogy determinant. Then the study on the SLJs was carried out by varying both macroscopic (bond length and thickness) and local (edge shape and angle) parameters for a

total of 30 cases. It was confirmed that the angle play an important party in reducing the singular stresses. Fig. 21 shows the finite element mesh of the joint.

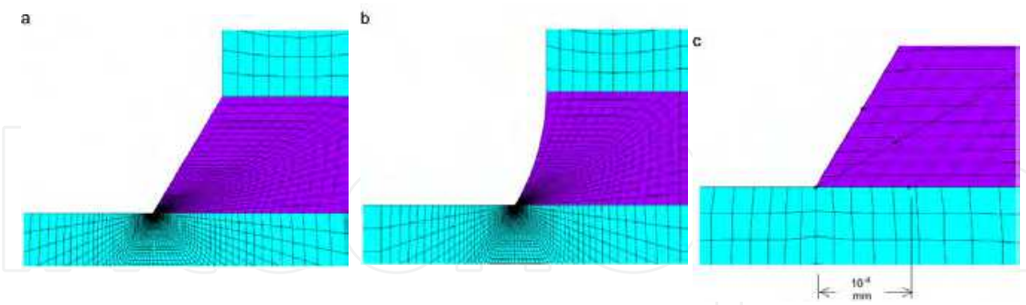

Fig. 21. Finite element mesh of the joint (Goglio & Rossetto, 2010): (a) straight edge; (b) fillet edge; (c) detail view of the elements near to the corner, representative of both cases (a) and (b).

4.1.3 Damage modeling

Damage modeling approach is being increasingly used to simulate fracture and debonding processes in adhesively bonded joints. The techniques for damage modeling can be divided into either local or continuum approaches. In the continuum approach the damage is modeled over a finite region. The local approach, where the damage is confined to zero volume lines and surfaces in 2-D and 3-D, respectively, is often referred to as cohesive zone approach.

Martiny et al. (Martiny et al., 2008) carried out numerical simulations of the steady-state fracture of adhesively bonded joints in various peel test configurations. The model was based on a multiscale approach involving the simulation of the continuum elasto-plastic response of the adherends and the adhesive layer, as well as of the fracture process taking place inside the adhesive layer using a cohesive zone formulation.

4.2 Environmental and fatigue behavior of adhesive bonded joints

Structural adhesives are generally thermosets such as acrylic, epoxy, polyurethane and phenolic adhesives. They will be affected by environmental conditions and exhibit time dependent characteristics. The lifetime of adhesive joints are difficult to model accurately and their long-term performance cannot easily and reliably be predicted, especially under the combined effects of an aggressive environment and fatigue loading (He, 2011b).

4.2.1 Moisture effects on adhesively bonded joints

The adhesives absorb moisture more than most substrate materials and expand more because of the moisture. Water may affect both the chemical and physical characteristics of adhesives and also the nature of the interfaces between adhesive and adherends.

Hua et al. (Hua et al., 2008) proposed a progressive cohesive failure model to predict the residual strength of adhesively bonded joints using a moisture-dependent critical equivalent plastic strain for the adhesive. A single, moisture-dependent failure parameter, the critical

strain, was calibrated using an aged, mixed-mode flexure (MMF) test. The FEA package ABAQUS was used to implement the coupled mechanical-diffusion analyses required. This approach has been extended to butt joints bonded with epoxy adhesive. This involves not only a different adhesive and joint configuration but the high hydro- static stress requires a more realistic yielding model (Hua et al., 2007).

4.2.2 Temperature effects on adhesively bonded joints

A detailed series of experiments and FEA were carried out by Grant et al. (Grant et al., 2009a) to assess the effects of temperature that an automotive joint might experience in service. Tests were carried out at -40 and +90 ^{0}C. It was shown that the failure criterion proposed at room temperature is still validat low and high temperatures, the failure envelope moving up and down as the temperature increases or decreases, respectively.

Apalak and Gunes (Apalak & Gunes, 2006) investigated 3D thermal residual stresses occurring in an adhesively bonded functionally graded SLJ subjected to a uniform cooling. They concluded that the free edges of adhesive–adherend interfaces and the corresponding adherend regions are the most critical regions, and the adherend edge conditions play more important role in the critical adherend and adhesive stresses.

4.2.3 Fatigue damage modeling

For adhesives, the presence of fatigue loading is found to lead to a much lower resistance to crack growth than under monotonic loading. The fatigue behavior of adhesively bonded joints needs a significant research improvement in order to understand the failure mechanisms and the influence of parameters such as surface pre-treatment, adhesive thickness or adherends thickness.

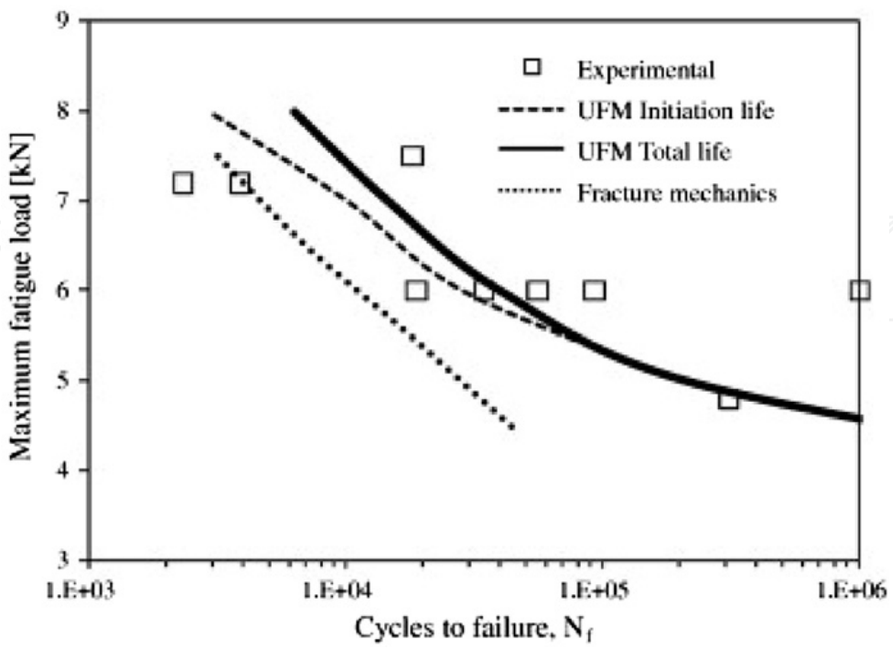

Fig. 22. Extended L–N curves using UFM and fracture mechanics (Shenoy et al., 2010).

A procedure to predict fatigue crack growth in adhesively bonded joints was developed by Pirondi and Moroni (Pirondi & Moroni, 2010) within the framework of Cohesive Zone Model (CZM) and FEA. The idea is to link the fatigue damage rate in the cohesive elements to the macroscopic crack growth rate through a damage homogenization criterion. In Shenoy et al.'s study (Shenoy et al., 2010), a unified fatigue methodology (UFM) was proposed to predict the fatigue behavior of adhesively bonded joints. In this methodology a damage evolution law is used to predict the main parameters governing fatigue life. The model is able to predict the damage evolution, crack initiation and propagation lives, strength and stiffness degradation and the backface strain (BFS) during fatigue loading. The model is able to unify previous approaches based on total life, strength or stiffness wearout, BFS monitoring and crack initiation and propagation modeling. Fig. 22 shows the extended L–N curve using UFM and fracture mechanics. It can be seen that the UFM approach, which accounts for both initiation and propagation can provide a good prediction of the total fatigue life at all loads.

4.3 Dynamic loading analysis of adhesive bonded joints

Adhesive bonding offers advantages on acoustic isolation and vibration attenuation relatively to other conventional joining processes. Mechanical structures assembled by adhesively bonding are expected to possess a high damping capacity because of the high damping capacity of the adhesives.

4.3.1 Structural damping

Investigations have been carried out for clarifying the damping characteristics of adhesively bonded structures and to establish an estimation method for the damping capacity. Research work by He (He, 2010a) studied the influence of adhesive layer thickness on the dynamic behavior of the single-lap adhesive joints. The results showed that the composite damping of the single-lap adhesive joint increases as the thickness of the adhesive layer increases.

In a research paper by Apalak and Yildirim (Apalak & Yildirim, 2007), the 3D transient vibration attenuation of an adhesively bonded cantilevered SLJ was controlled using actuators. The transient variation of the control force was expressed by a periodic function so that the damped vibration of the SLJ was decreased. Optimal transient control force history and optimal actuator position were determined using the Open Loop Control Approach (OLCA) and Genetic Algorithm.

4.3.2 Modes of vibration

With the increase in the use of adhesively bonded joints in primary structures, such as aircraft and automotive structures, reliable and cost-effective techniques for structural health monitoring (SHM) of adhesive bonding are needed. Modal and vibration-based analysis, when combined with validated FEA, can provide a key tool for SHM of adhesive bonding.

Gunes et al. (Gunes et al., 2010) investigated the free vibration behavior of an adhesively bonded functionally graded SLJ, which composed of ceramic (Al2O3) and metal (Ni) phases

varying through the plate thickness. The effects of the similar and dissimilar material composition variations through-the-thicknesses of both upper and lower plates on the natural frequencies and corresponding mode shapes of the adhesive joint were investigated using both the FEA and the back-propagation artificial neural network (ANN) method. A series of the free vibration analyses were carried out for various random values of the geometrical parameters and the through-the-thickness material composition so that a suitable ANN model could be trained successfully.

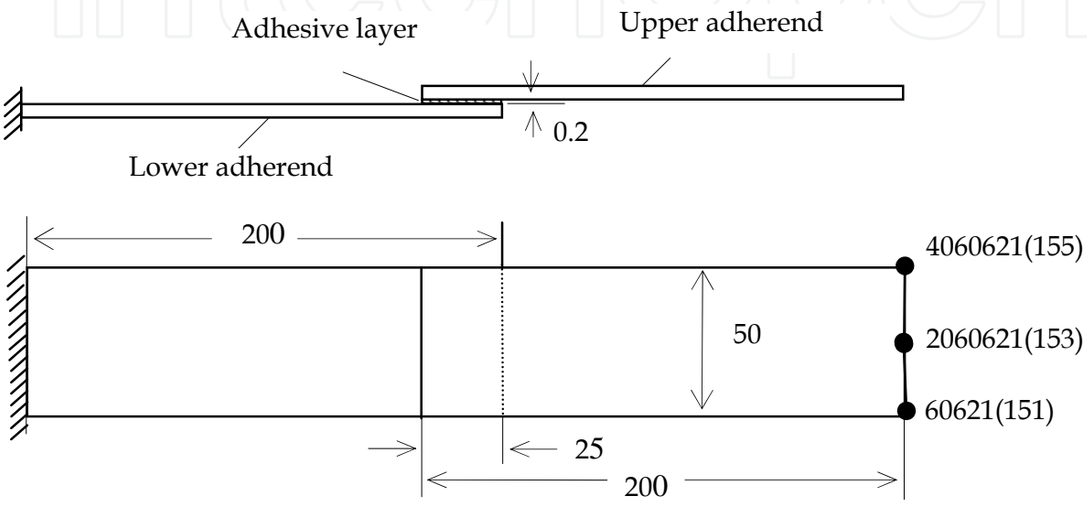

Fig. 23. Location of nodes at the free edge of the beam (He, 2009).

The ABAQUS FEA software was used by He (He, 2009) to predict the natural frequencies, mode shapes and frequency response functions (FRFs) of adhesively lap-jointed beams. In the case of forced vibration of the single lap-jointed cantilevered beam, some typical points on the free edge were chosen for response points because they can better represent the dynamical characteristic of the beams. Nodes 151, 153 and 155 in Fig. 23 are the nodes at the two corners and center of the free edge of the beam (the corresponding nodes in the FE mesh are 60621, 2060621 and 4060621, respectively).

The overlay of the FRFs predicted using FEA and measured experimentally at the 2 corners and centre of the free edge of the beam are shown in Fig. 24. It can be seen that the measued FRFs are close to the predicted FRFs for the first few modes of vibration of the beam. For the higher order modes of vibration, there is considerable discrepancy between the measured and predicted FRFs. This discrepancy can be attributed to locations and additional masses of force transducer and accelerometer. In order to fully excite the beams, the force transducer was connected to the location which was 20% of the length of the beam from the clamped end and very close to a free edge. The accelerometer was connected to different locations of the beam for obtaining precise mode shapes. As a result, the natural frequencies from experiments are lower than those predicted using FEA and some complexity appear in the FRFs graphics.

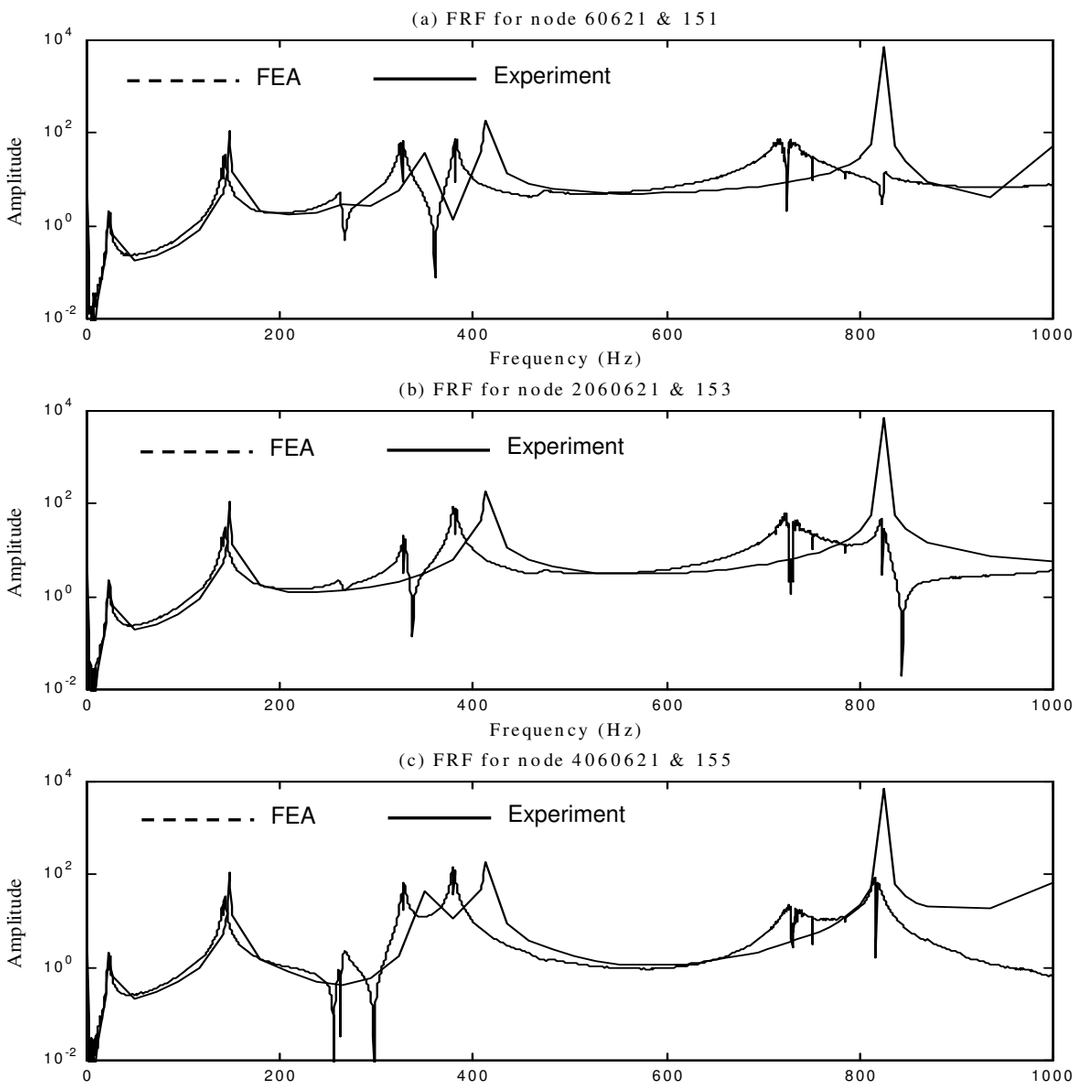

Fig. 24. FRFs predicted by FEA and measured using the test rig (He, 2009).

5. FEA of hybrid joints

It is also important for one joining process to benefit from the advantages of other joining techniques. These can be done by combining one joining process with other joining techniques and are referred to as hybrid joining processes. A number of researchers have carried out mechanical performances of the hybrid joints in different materials with various load conditions. Their study shows that the combination produced a much stronger joint in both static and fatigue tests.

5.1 Clinch-bonded hybrid joints

Pirondi and Moroni (Pirondi & Moroni, 2009) simulated the failure behavior of clinch-bonded and rivet-bonded hybrid joints using the FEA. The analyses were conducted using

Arbitrary Lagrangian–Eulerian (ALE) adaptive meshing to avoid excessive element distortion and mass scaling to increase the minimum time increment in explicit analyses. The authors concluded that different damage models, tuned with experiments performed on simple joints (riveted, clinched or adhesively bonded), can be combined in a unique model to simulate effectively the failure behavior of hybrid joints. A detailed series of tests and FEA were conducted by Grant et al. (Grant et al., 2009b) for clinch-bonded hybrid joints. The experimental results were compared with spot welded joints and adhesively bonded double-lap joints. It was concluded that this joint fails because of large plastic deformation in the adherend. By means of 3D ANSYS FEA, the influence of Young's modulus and Poisson's ratio of the structural adhesives on the natural frequencies, natural frequency ratios, and mode shapes of the single-lap clinch-bonded hybrid joints was deduced by He et al. (He et al., 2010b).

5.2 SPR-bonded hybrid joints

The torsional free vibration behavior of SLJ encastre hybrid SPR-bonded beams has been studied by He et al. (He et al., 2009b) using the commercially available ANSYS FEA program. The mode shapes showed that there are different deformations in the jointed section of the odd and even modes. These different deformations may result different dynamic response and different stress distributions. Another research work by the same authors investigated in detail the free transverse vibration characteristics of single-lap SPR-bonded hybrid joints (He et al., 2010a). The FEA results showed that the stiffer adhesive is likely to suffer fatigue failure and debonding more often than the softer adhesive. These deformations may result in relatively high stresses in the adhesive layers and initiate local cracking and delamination failures.

6. Conclusions

Some joining techniques have become increasingly popular alternatives to traditional spot welding due to the growing use of alternative materials which are difficult or impossible to weld. Adequate understanding of the behavior of joints is necessary to ensure efficiency, safety and reliability of such joining structures. However, accurate and reliable modeling of joining structures is still a difficult task as the mechanical behavior of these joints is not only influenced by the geometric characteristics of the joint but also by different factors and their combinations.

The information that can be obtained from the FEA of sheet material joints includes: differences in the basic mechanical properties, hygrothermal behavior, occurrences of high stress gradients in certain regions of the joints. An accurate FEA model of sheet material joint must be able to predict failure in the substrates and at the interfaces, and must also account for full non-linear material behavior.

In this chapter the research and progress in FEA of sheet material joints are critically reviewed and current trends in the application of FEA are mentioned. It is concluded that the FEA of sheet material joints will help future applications of sheet material joining by allowing different parameters to be selected to give as large a process window as possible for joint manufacture. This will allow many tests to be simulated that would currently take too long to perform or be prohibitively expensive in practice, such as modifications to geometry or material properties.

7. Acknowledgment

This study is partially supported by National Science Foundation of China (Grant No. 50965009).

8. References

Abe, Y.; Kato, T. & Mori, K. (2006). Joinability of aluminum alloy and mild steel sheets by self piercing rivet. *Journal of Materials Processing Technology,* Vol. 177, No. 1-3, (July 2006), pp. 417-421, ISSN 0924-0136

Abe, Y.; Kato, T. & Mori, K. (2009). Self-piercing riveting of high tensile strength steel and aluminum alloy sheets using conventional rivet and die. *Journal of Materials Processing Technology,* Vol. 209, No. 8, (April 2009), pp. 3914-3922, ISSN 0924-0136

Apalak, M. K. &; Gunes, R. (2006). Thermal residual stresses in an adhesively-bonded functionally graded single-lap joint. *Journal of Adhesion Science and Technology,* Vol. 20, No. 12, (December 2006), pp. 1295-1320, ISSN 0169-4243

Apalak, M. K. & Yildirim, M. (2007). Optimal vibration attenuation of an adhesively-bonded cantilevered single-lap joint. *Journal of Adhesion Science and Technology,* Vol. 21, No. 3-4, (April 2007), pp. 267-286, ISSN 0169-4243

Atzeni, E.; Ippolito, R. & Settineri, L. (2007). FEM modeling of self-piercing riveted joint. *Key Engineering Materials,* Vol. 344, (July 2007), pp. 655–662, ISSN 1013-9826

Atzeni, E.; Ippolito, R. & Settineri, L. (2009). Experimental and numerical appraisal of self-piercing riveting. *CIRP Annals - Manufacturing Technology,* Vol. 58, No. 1, (December 2009), pp. 17-20, ISSN 0007-8506

Borsellino, C.; Di Bella, G. & Ruisi, V.F. (2007). Study of new joining technique: flat clinching. *Key Engineering Materials,* Vol. 344, (July 2007), pp. 685–692, ISSN 1013-9826

Bouchard, P.O.; Laurent, T. & Tollier, L. (2008). Numerical modeling of self-pierce riveting—from riveting process modeling down to structural analysis. *Journal of Materials Processing Technology,* Vol. 202, No. 1-3, (June 2008), pp. 290–300, ISSN 0924-0136

Cai, W.; Wang, P. & Yang, W. (2005). Assembly dimensional prediction for self-piercing riveted aluminium panels. *International Journal of Machine Tools and Manufacture*, Vols. 45, No. 6, (May 2005), pp. 695-704, ISSN 0890-6955

Carboni, M.; Beretta, S. & Monno, M. (2006). Fatigue behavior of tensile-shear loaded clinched joints. *Engineering Fracture Mechanics,* Vol. 73, No. 2, (January 2006), pp. 178-190, ISSN 0013-7944

Casalino, G.; Rotondo, A. & Ludovico, A. (2008). On the numerical modeling of the multiphysics self piercing riveting process based on the finite element technique. *Advanced Engineering Software,* Vol. 39, No. 9, (September 2008), pp. 787-795, ISSN 0965-9978

de Paula, A.A.; Aguilar, M.T.P.; Pertence, A.E.M. & Cetlin, P.R. (2007). Finite element simulations of the clinch joining of metallic sheets. *Journal of Materials Processing Technology,* Vol. 182, No. 1-3, (February 2007), pp. 352–357, ISSN 0924-0136

Dong, B. ; He, X. & Zhang, W. (2010). Harmonic response analysis of single lap self-piercing riveted joints. *New Technology & New Process (in Chinese),* Vol. 275, (November 2010), pp. 51-54, ISSN 1003-5311

Feng, M. ; He, X. ; Yan K. & Zhang, Y. (2011). Numerical simulation and analysis of clinch process. *Science Technology and Engineering (in Chinese),* Vol. 11, No. 23, (August 2011), pp. 5538-5541, ISSN 1671-1815

Galtier, A. & Duchet, M. (2007). Fatigue behaviour of high strength steel thin sheet assemblies. *Welding in the World,* Vol. 51, No. 3-4, (March/April 2007), pp. 19-27, ISSN 0043-2288

Gao, S. & He, X. (2010). Influence of adhesive characteristics on transverse free vibration of single lap clinched joints. *Machinery (in Chinese),* Vol. 48, No. 553, (September 2010), pp. 32-34, ISSN 1000-4998

Goglio, L. & Rossetto, M. (2010). Stress intensity factor in bonded joints: Influence of the geometry, *International Journal of Adhesion and Adhesives,* Vol. 30, No. 5, (July 2010), pp. 313-321, ISSN 0143-7496

Grant, L.D.R.; Adams, R.D. & da Silva, L.F.M. (2009a). Effect of the temperature on the strength of adhesively bonded single lap and T joints for the automotive industry. *International Journal of Adhesion and Adhesives,* Vol. 29, No. 5, (July 2009), pp. 535-542, ISSN 0143-7496

Grant, L.D.R.; Adams, R.D. & da Silva, L.F.M. (2009b). Experimental and numerical analysis of clinch (hemflange) joints used in the automotive industry. *Journal of Adhesion Science and Technology,* Vol. 23, No. 12, (September 2009), pp. 1673-1688, ISSN 0169-4243

Gunes, R.; Apalak, M.K. Yildirim, M. & Ozkes, I. (2010). Free vibration analysis of adhesively bonded single lap joints with wide and narrow functionally graded plates. *Composite Structures,* Vol. 92, No. 1, (January 2010), pp. 1-17, ISSN 0263-8223

Hamel, V.; Roelandt, J.M.; Gacel, J.N. & Schmit, F. (2000). Finite element modeling of clinch forming with automatic remeshing. *Computers and Structures,* Vol. 77, No. 2, (June 2000), pp. 185-200, ISSN 0045-7949

He, X.; Pearson, I. & Young, K. (2006). Free vibration characteristics of SPR joints. *Proceedings of 8th Biennial ASME Conference on Engineering Systems Design and Analysis,* pp. 1-7, ISBN_10 0791837793, Torino, Italy, July 4-7, 2006

He, X.; Pearson, I. & Young, K. (2007). Three dimensional finite element analysis of transverse free vibration of self-pierce riveting beam. *Key Engineering Materials,* Vol. 344, (July 2007), pp. 647–654, ISSN 1013-9826

He, X.; Pearson, I. & Young, K. (2008). Self-pierce riveting for sheet materials: State of the art. *Journal of Materials Processing Technology,* Vol.199, No.1-3, (April 2008), pp. 27-36, ISSN 0924-0136

He, X. (2009). Dynamic behaviour of single lap-jointed cantilevered beams. *Key Engineering Materials,* Vols. 413-414, (August 2009), pp. 733-740, ISSN 1013-9826

He, X.; Zhang, W.; Dong, B. Zhu, X. & Gao, S. (2009a). Free vibration characteristics of clinched joints. *Lecture Notes in Engineering and Computer Science*, Vol. 1, (July 2009), pp. 1724-1729, ISBN 978-988-18210-1-0

He, X. ; Dong, B. & Zhu, X. (2009b). Free Vibration Characteristics of Hybrid SPR Beams, *AIP Conference Proceedings* Vol. 1233, pp. 678-683, ISBN 978-0-7354-0778-7, Hong Kong-Macau, China, November 30-Desember 3, 2009

He, X. (2010a). Bond Thickness Effects upon Dynamic Behavior in Adhesive Joints. *Advanced Materials Research*, Vols. 97-101 (April 2011), pp. 3920-3923, ISSN 1022-6680

He, X. (2010b). Recent development in finite element analysis of clinched joints. *International Journal of Advanced Manufacturing Technology,* Vol. 48, (May 2010), pp. 607-612, ISSN 0268-3768

He, X.; Zhu, X. & Dong, B. (2010a). Transverse free vibration analysis of hybrid SPR steel joints. Proceedings of MIMT 2010, p 389-394, ISBN-13: 9780791859544, Sanya, China, January 22-24, 2010

He, X.; Gao, S. & Zhang, W. (2010b). Torsional free vibration characteristics of hybrid clinched joints. *Proceedings of ICMTMA 2010,* Vol. 3, pp. 1027-1030, ISBN-13: 9780769539621, Changsha, China, March 13-14, 2010

He, X. (2011a). Stress Distribution of Bonded Joint with Rubbery Adhesives. *Advanced Materials Research*, Vols. 189-193 (April 2011), pp 3427-3430, ISSN 1022-6680

He, X. (2011b). A review of finite element analysis of adhesively bonded joints. *International Journal of Adhesion and Adhesives,* Vol. 31, No. 4, (June 2011), pp. 248-264, ISSN 0143-7496

He, X. (2011c). Comparisons of finite element models of bonded joints. *Applied Mechanics and Materials,* Vols. 66-68, (September 2011), pp. 2192-2197, ISSN 1660-9336

He, X. (2012). Recent development in finite element analysis of self-piercing riveted joints. *International Journal of Advanced Manufacturing Technology,* Vol. 58, (January 2012), pp. 643-649, ISSN 0268-3768

Hoang, N.H.; Porcaro, R.; Langseth, M. & Hanssen, A.G. (2010). Self-piercing riveting connections using aluminum rivets. *International Journal of Solids and Structure,* Vols. 47, No. (3–4), (February 2010), pp. 427–439, ISSN 0020-7683

Hua, Y.; Crocombe, A.D.; Wahab, M.A. & Ashcroft, I.A. (2007). Continuum damage modelling of environmental degradation in joints bonded with E32 epoxy adhesive. *Journal of Adhesion Science and Technology,* Vol. 21, No. 2, (February 2008), pp. 179-195, ISSN 0169-4243

Hua, Y.; Crocombe, A.D.; Wahab, M.A. & Ashcroft, I.A. (2008). Continuum damage modelling of environmental degradation in joints bonded with EA9321 epoxy adhesive. *International Journal of Adhesion and Adhesives,* Vol. 28, No. 6, (September 2008), pp. 302-313, ISSN 0143-7496

Iyer, K.; Hu, S.J.; Brittman, F.L.; Wang, P.C.; Hayden, D.B. & Marin, S.P. (2005). Fatigue of single- And double-rivet self-piercing riveted lap joints. *Fatigue and Fracture of Engineering Materials and Structures,* Vol. 28, No. 11, (November 2005), pp. 997-1007, ISSN 1460-2695

Kato, T.; Abe, Y. & Mori, K. (2007). Finite element simulation of self-piercing riveting of three aluminum alloy sheets. *Key Engineering Materials,* Vols. 340-341, (July 2007), pp. 1461-1466, ISSN 1013-9826

Kilic, B.; Madenci, E. & Ambur, D.R. (2006). Influence of adhesive spew in bonded single-lap joints, *Engineering Fracture Mechanics,* Vol. 73, No. 11, (July 2006), pp. 1472-1490, ISSN 0013-7944

Kim, M.G.; Kim, J.H.; Lee, K.C. & Yi, W. (2005). Assessment for structural stiffness and fatigue life on self-piercing rivet of car bodies. *Key Engineering Materials,* Vols. 297-300, (July 2005), pp. 2519-2524, ISSN 1013-9826

Lennon, R.; Pedreschi, R. & Sinha, B.P. (1999). Comparative study of some mechanical connections in cold formed steel. *Construction and Building Materials,* Vol. 13, No. 3, (April 1999), pp. 109-116, ISSN 0950-0618

Lim, B. K. (2008). Analysis of fatigue life of SPR(Self-Piercing Riveting) jointed various specimens using FEM. *Materials Science Forum,* Vols. 580-582, (July 2008), pp. 617-620, ISSN 0255-5476

Martiny, Ph.; Lani, F.; Kinloch, A.J. & Pardoen, T. (2008). Numerical analysis of the energy contributions in peel tests: A steady-state multilevel finite element approach. *International Journal of Adhesion and Adhesives,* Vol. 28, No. 4-5, (June 2008), pp. 222-236, ISSN 0143-7496

Mori, K.; Kato, T.; Abe, Y. & Ravshanbek, Y. (2006). Plastic joining of ultra high strength steel and aluminum alloy sheets by self piercing rivet. *CIRP Annals - Manufacturing Technology,* Vol. 55, No. 1, (December 2006), pp. 283-286, ISSN 0007-8506

Neugebauer, R.; Kraus, C. & Dietrich, S. (2008) Advances in mechanical joining of magnesium. *CIRP Annals - Manufacturing Technology,* Vol. 57, No. 1, (December 2008), pp. 283-286, ISSN 0007-8506

Oudjene, M. & Ben-Ayed, L. (2008). On the parametrical study of clinch joining of metallic sheets using the Taguchi method. *Engineering Structures,* Vol. 30, No. 6, (June 2008), pp. 352–357, ISSN 0141-0296

Oudjene, M.; Ben-Ayed, L.; Delamézière, A. & Batoz, J.L. (2009). Shape optimization of clinching tools using the response surface methodology with moving least-square approximation. *Journal of Materials Processing Technology,* Vol. 209, No.1, (January 2009), pp. 289–296, ISSN 0924-0136

Pirondi, A. & Moroni, F. (2009). Clinch-bonded and rivet-bonded hybrid joints: Application of damage models for simulation of forming and failure. *Journal of Adhesion Science and Technology,* Vol. 23, No. 10-11, (July 2009), pp. 1547-1574, ISSN 0169-4243

Pirondi, A. & Moroni, F. (2010). A progressive damage model for the prediction of fatigue crack growth in bonded joints. *Journal of Adhesion,* Vol. 86, No. 5-6, (April 2010), pp. 501-521, ISSN 0021-8464

Porcaro, R.; Hanssen, A.G.; Aalberg, A. & Langseth, M. (2004). Joining of aluminum using self-piercing riveting: Testing, modeling and analysis. *International Journal of Crashworthiness,* Vol. 9, No. 2, (May 2004), pp. 141–154, ISSN 1358-8265

Porcaro, R.; Hanssen, A.G.; Langseth, M. & Aalberg, A. (2006). The behaviour of a self-piercing riveted connection under quasi-static loading conditions. *International Journal of Solids and Structure,* Vols. 43, No. 17, (August 2006), pp. 5110-5131, ISSN 0020-7683

Porcaro, R.; Langseth, M.; Hanssen, A.G.; Zhao, H.; Weyer, S. & Hooputra, H. (2008). Crashworthiness of self-piercing riveted connections. *International Journal of Impact Engineering,* Vols. 35, No. 11, (November 2008), pp. 1251-1266, ISSN 0734-743X

Shenoy, V.; Ashcroft, I.A.; Critchlow, G.W. & Crocombe, A.D. (2010). Unified methodology for the prediction of the fatigue behaviour of adhesively bonded joints. *International Journal of Fatigue,* Vol. 32, No. 8, (August 2010), pp. 1278-1288, ISSN 0142-1123

Speth, D.R.; Yang, Y. & Ritter, G.W. (2010). Qualification of adhesives for marine composite-to-steel applications. *International Journal of Adhesion and Adhesives,* Vol. 30, No. 2, (March 2010), pp. 55-62, ISSN 0143-7496

Sui, B.; Du, D.; Chang, B.; Huang, H. & Wang, L. (2007). Simulation and analysis of self-piercing riveting process in aluminum sheets. *Material Science and Technology (in Chinese),* Vol. 15, No. 5, (October 2007), pp. 713-717, ISSN 1005-0299

Varis, J.P. & Lepistö, J. (2003). A simple testing-based procedure and simulation of the clinching process using finite element analysis for establishing clinching parameters. *Thin-Walled Structures,* Vol. 41, No. 8, (August 2003), pp. 691-709, ISSN 0263-8231

Yan, k.; He, X. & Zhang, Y. (2011). Numerical simulation and quality evaluation of single lap self-piercing rivetiong process. *China Manufacturing Information (in Chinese),* Vol. 40, No. 19, (October 2011), pp. 76-78, ISSN 1672-1616

Zhang, W.; He, X. & Dong, B. (2010). Analysis of harmonic response of single lap clinched joints. *Machinery (in Chinese),* Vol. 48, No. 555, (November 2010), pp. 19-21, ISSN 1000-4998

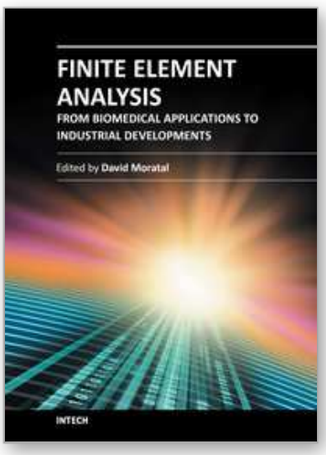

Finite Element Analysis - From Biomedical Applications to Industrial Developments

Edited by Dr. David Moratal

ISBN 978-953-51-0474-2
Hard cover, 496 pages
Publisher InTech
Published online 30, March, 2012
Published in print edition March, 2012

Finite Element Analysis represents a numerical technique for finding approximate solutions to partial differential equations as well as integral equations, permitting the numerical analysis of complex structures based on their material properties. This book presents 20 different chapters in the application of Finite Elements, ranging from Biomedical Engineering to Manufacturing Industry and Industrial Developments. It has been written at a level suitable for use in a graduate course on applications of finite element modelling and analysis (mechanical, civil and biomedical engineering studies, for instance), without excluding its use by researchers or professional engineers interested in the field, seeking to gain a deeper understanding concerning Finite Element Analysis.

How to reference

In order to correctly reference this scholarly work, feel free to copy and paste the following:

Xiaocong He (2012). Application of Finite Element Analysis in Sheet Material Joining, Finite Element Analysis - From Biomedical Applications to Industrial Developments, Dr. David Moratal (Ed.), ISBN: 978-953-51-0474-2, InTech, Available from: http://www.intechopen.com/books/finite-element-analysis-from-biomedical-applications-to-industrial-developments/application-of-finite-element-analysis-in-sheet-material-joining

INTECH
open science | open minds

InTech Europe
University Campus STeP Ri
Slavka Krautzeka 83/A
51000 Rijeka, Croatia
Phone: +385 (51) 770 447
Fax: +385 (51) 686 166
www.intechopen.com

InTech China
Unit 405, Office Block, Hotel Equatorial Shanghai
No.65, Yan An Road (West), Shanghai, 200040, China
中国上海市延安西路65号上海国际贵都大饭店办公楼405单元
Phone: +86-21-62489820
Fax: +86-21-62489821

IntechOpen